

SPH NUMERICAL AND PHYSICAL MODELING OF WAVE OVERTOPPING A POROUS BREAKWATER

ERIC DIDIER⁽¹⁾, DIOGO NEVES⁽¹⁾ PAULO TEIXEIRA⁽²⁾,
JOÃO DIAS⁽¹⁾ & MARIA G. NEVES⁽¹⁾

⁽¹⁾ National Laboratory of Civil Engineering, Lisbon, Portugal
edidier@lnec.pt, dneves@lnec.pt, jdias@lnec.pt, gneves@lnec.pt

⁽²⁾ Federal University of Rio Grande, Rio Grande, Rio Grande do Sul, Brazil
pauloteixeira@furg.br

Abstract

Numerical modeling of an entire physical wave flume with a breakwater at scale 1:30 was performed using a coupling technique between FLUINCO wave propagation and SPHyCE wave-structure interaction codes. The rock blocks of the breakwater are directly simulated with the SPHyCE code using similar rectangular blocks. Numerical results of free surface elevation before the breakwater, over and inside the rock armor layer and overtopping discharge over the structure, for wave period 12s and wave heights 2.5 and 3.3m (prototype values), are in good accordance with experimental data.

Keywords: Overtopping, Smoothed Particle Hydrodynamics, Physical modeling, Porous breakwater

1. Introduction

The Smoothed Particle Hydrodynamics numerical model SPHyCE allows simulating complex non-linear flows produced by the interaction between waves and coastal structures, such as wave breaking, impact loads and wave overtopping.

Within the objective of validating the numerical model SPHyCE for porous coastal structures, a 1:30 scale physical model of a breakwater section was performed on a wave flume at LNEC (Laboratório Nacional de Engenharia Civil). As SPHyCE model is not able to simulate the entire flume due to its high CPU time, a passive coupling technique between two numerical models was developed: wave propagation, in the first part of the flume, was modeled using the FLUINCO mesh-based code (Teixeira and Awruch, 2005; Teixeira and Fortes, 2009); and in the second part of the flume, wave interaction with the breakwater was modeled using SPHyCE code (Didier and Neves, 2012; Neves et al., 2012; Didier et al., 2013). The passive coupling approach consists in transferring the wave characteristics in a section of the wave flume from FLUINCO to SPHyCE numerical model.

This paper presents the two numerical codes, the experimental set-up and the coupling technique. The models were applied for the experimental tests performed in the physical wave flume with a porous breakwater for a tide level of +3.5m (CD) (Chart Datum), a wave period of 12s and wave heights of 2.5m and 3.3m (at prototype values). Numerical results of free surface elevation before, over and inside the rock armor layer and overtopping discharge over the structure were compared with experimental data.

2. Coupling technique between FLUINCO and SPHyCE numerical models

The two numerical models, SPHyCE and FLUINCO, and the passive coupling technique based on these two codes are here presented and explained.

2.1 FLUINCO wave propagation model

FLUINCO code is based on a finite element method and allows modeling wave propagation (Teixeira and Awruch, 2005; Teixeira and Fortes, 2009). Numerical procedure is described and consists basically of four principal steps.

Non-corrected velocity \tilde{U}_i is calculated at $t+\Delta t/2$, where the pressure term is at instant t :

$$\tilde{U}_i^{n+1/2} = U_i^n - \frac{\Delta t}{2} \left(\frac{\partial f_{ij}^n}{\partial x_j} - \frac{\partial \tau_{ij}^n}{\partial x_j} + \frac{\partial p^n}{\partial x_i} - \rho g_i - w_j^n \frac{\partial U_i^n}{\partial x_i} \right) \quad [1]$$

where ρ is the specific mass, p is the pressure, g_i are the gravity acceleration components, w_i are the velocity components of the reference system and τ_{ij} is the viscous stress tensor, $U_i = \rho v_i$, $f_{ij} = v_j(\rho v_i) = v_j U_i$ and v_i are the velocity components ($i, j = 1, 2$).

The pressure p is updated at $t+\Delta t$ and given by the Poisson equation:

$$\frac{1}{c^2} \Delta p = -\Delta t \left[\frac{\partial \tilde{U}_i^{n+1/2}}{\partial x_i} - \frac{\Delta t}{4} \frac{\partial}{\partial x_i} \frac{\partial \Delta p}{\partial x_i} \right] \quad [2]$$

where $\Delta p = p^{n+1} - p^n$ and $i = 1, 2$.

The velocity is corrected at $t+\Delta t/2$, adding the pressure variation term from t to $t+\Delta t/2$, according to the equation:

$$U_i^{n+1/2} = \tilde{U}_i^{n+1/2} - \frac{\Delta t}{4} \frac{\partial \Delta p}{\partial x_i} \quad [3]$$

The velocity at $t+\Delta t$ is calculated using variables updated in the previous steps as follows:

$$U_i^{n+1} = U_i^n - \Delta t \left(\frac{\partial f_{ij}^{n+1/2}}{\partial x_j} - \frac{\partial \tau_{ij}^{n+1/2}}{\partial x_j} + \frac{\partial p^{n+1/2}}{\partial x_i} - w_j^{n+1/2} \frac{\partial U_i^{n+1/2}}{\partial x_i} - \rho g_i \right) \quad [4]$$

The classical Galerkin weighted residual method is applied to the space discretization of Eq. [1], [2], [3] and [4], and a triangular element is employed. In the variables at $t+\Delta t/2$ instant, a constant shape function is used, and in the variables at t and $t+\Delta t$, a linear shape function is employed (Teixeira and Awruch, 2001).

FLUINCO model assumes the free surface subjected to a constant atmospheric pressure and imposes the free surface kinematic boundary condition (KBC), using the Arbitrary Lagrangian Eulerian (ALE) formulation expressed as:

$$\frac{\partial \eta}{\partial t} + \left({}^{(s)}v_i - {}^{(s)}w_i \right) \frac{\partial \eta}{\partial x_i} = 0 \quad \text{with } (i = 1, 2, 3) \quad [5]$$

where η is the free surface elevation, ${}^{(s)}v_i$ and ${}^{(s)}w_i$ are fluid and mesh velocity components in the free surface, respectively. An Eulerian formulation is used for x and y direction on the horizontal plane and an ALE formulation is employed to z direction. The temporal discretization of the KBC is made in the same way as in the momentum equations, using boundaries of the triangle that belong to the free surface. The spatial distribution of the mesh velocity minimizes the element distortions through a weight functions.

2.2 SPHyCE wave-structure interaction model

SPHyCE is a code that uses two-dimensional SPH equations based on the Lagrangian formulation of the conservation of momentum and continuity for a viscous fluid, written as:

$$\frac{dv}{dt} = -\frac{1}{\rho} \nabla P + \Pi + g \quad \text{and} \quad \frac{1}{\rho} \frac{d\rho}{dt} = -\text{div}(v) \quad [6]$$

where t is the time, Π represents the viscous terms, $g = (0, -9.81)\text{ms}^{-2}$ is the acceleration of gravity, v , P and ρ are the velocity, pressure and density, respectively.

The standard SPH formulation (Monaghan, 1994), in which the fluid is treated as weakly-compressible, allows calculating the pressure by an equation of state (Batchelor, 1974):

$$P = B \left[\left(\frac{\rho}{\rho_0} \right)^\gamma - 1 \right] \quad \text{with} \quad B = \frac{c_0^2 \rho_0}{\gamma} \quad [7]$$

with $\gamma=7$, ρ_0 the reference density (for water: $1000\text{kg}\cdot\text{m}^{-3}$) and c_0 the sound velocity.

The trajectories of the particles are obtained from the following relationship.

$$\frac{dr}{dt} = v \quad [8]$$

SPHyCE numerical model, based on the SPHysics code (Gómez-Gesteira *et al.*, 2008, 2010), version 1.4 (SPHysics code, version 1.4, 2008), has been developed and improved for specifically solving coastal engineering problems and modeling complex free surface flows and wave interaction with coastal structures (impermeable and porous structures).

For numerical simulations of wave propagation and interaction with a coastal structure, the quadratic kernel (Johnson *et al.*, 1996) is used to determine the interaction between particles.

The Sub-Particle Scale (SPS) laminar viscosity turbulence model (Gotoh *et al.*, 2001; Rogers and Dalrymple, 2004) is used because it includes not only a model of laminar viscosity but also the effects related to the turbulence through a model derived from the Large Eddy Simulation.

Integration in time is performed by the Predictor-Corrector model using a variable time step to ensure the CFL condition.

The boundary conditions are not displayed directly in the SPH formalism. In the present model the repulsive boundary condition Monaghan and Kos (1999), that imposes a repulsive force to the fluid particles from the boundary particles, is used. Nevertheless, some improvements were made in SPHyCE for preventing the water particles to cross the boundary.

In order to simulate a semi-infinite numerical wave flume, a piston-type wave-maker active absorption was implemented in SPHyCE model (Didier and Neves, 2012). This numerical wave-maker is equipped with a control system for simultaneous wave generation and active wave absorption of the reflected waves. Without the undesired influence of re-reflection of waves at the wave-maker, the control enables to obtain longer time series of free surface elevation, overtopping and forces that are needed for a correct calculation of the statistical parameters. The active wave-maker absorption includes also the correction of the paddle drift in order to maintain the initial average position of the wave-maker (Neves *et al.*, 2012).

A technique of semi-automatic refinement was also implemented in the model. This technique, based on the division of fluid particles, improves significantly both the accuracy of solution and allows reducing the computational time from 35 to 47%.

Initially, the water particles are placed in the flume using a regular Cartesian grid with spacing between particles defined by d_0 . The velocity field is zero and the pressure is hydrostatic.

The detailed description of the numerical implementation is available in (Gómez-Gesteira *et al.*, 2008, 2010; SPHysics code v1.4, 2008; Didier and Neves, 2012, 2013; Neves *et al.*, 2012).

2.3 Coupling technique between FLUINCO and SPHyCE

The passive coupling method between FLUINCO and SPHyCE was developed for incident regular waves. Figure 1 shows a scheme of the simulated domain and the two numerical sub-domains that correspond to the application of each code.

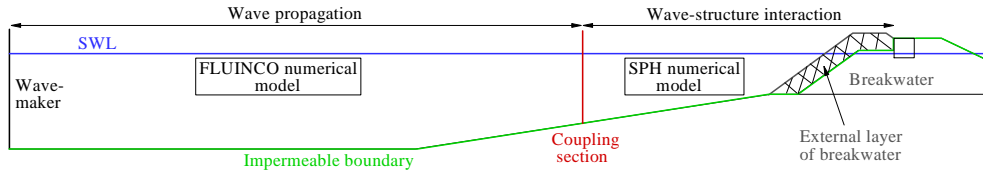


Figure 1. Entire computational domain with the respective domains of application of each code and the position of the coupling section.

The wave propagation was modeled with FLUINCO considering the flume without the breakwater, in order to obtain the time series of the free surface elevation at the coupling section without reflected waves from the structure, afterwards a spectral analysis of the time series using the Discrete Fourier Transform (DFT) was performed. Relative amplitude $a^{(n)}$ and phase $\theta^{(n)}$ of fundamental and harmonic frequencies of the incident wave at the coupling section were defined.

Considering the water depth at the coupling section, i.e., at the SPHyCE wave-maker section, the amplitude of the wave-maker, $A_b^{(n)}$, was calculated from the wave amplitude, $a^{(n)}$ of each frequency $f^{(n)}$, obtained from FLUINCO. Motion of wave-maker was defined as the sum of the contribution of the relevant frequencies, as follow:

$$X_b(t) = \sum_n A_b^{(n)} \cos(2\pi t/T^{(n)} + \theta^{(n)}) \quad [9]$$

The generated wave at the wave-maker was composed by the sum of the relevant frequencies:

$$\eta_b(t) = \sum_n a^{(n)} \sin(2\pi t/T^{(n)} + \theta^{(n)}) \quad [10]$$

These wave characteristics were reproduced in the SPHyCE by a piston-type wave-maker motion that includes absorption of the reflected waves for the modeling of the interaction between the transformed incident wave and the breakwater. The SPHyCE numerical domain was short and the distance between wave-maker and breakwater was less than one wave length. The coupling technique can also be applied between the experimental data and the SPHyCE code. From the measured time series of free surface elevation in a section of the flume, the coupling method allows to impose the same incident wave. However, tests without the breakwater had to be done in order to have the incident wave characteristics without the effect of structure reflection.

3. Physical modeling

The experimental tests of the wave propagation and interaction with a porous breakwater were performed for a section of the west breakwater of the Albufeira harbor, Figure 2, at scale 1:30, in a wave flume at LNEC (Laboratório Nacional de Engenharia Civil) with 49.4m length and 1.6m wide. The modeled bathymetry was based on the bottom near the studied section of the breakwater, characterized by a horizontal zone of 23.04m and, before the structure, a 13.96m ramp with a 2.1% slope. The toe of the structure was located at 37.0m from the piston type wave-maker. The water level at the wave-maker for all the experiments was 0.51m, corresponding to 0.217m at the toe of the structure, which represents, in prototype, a tide level of +3.5m (CD) (Chart Datum). Figure 2 shows the flume profile and the principal dimensions.

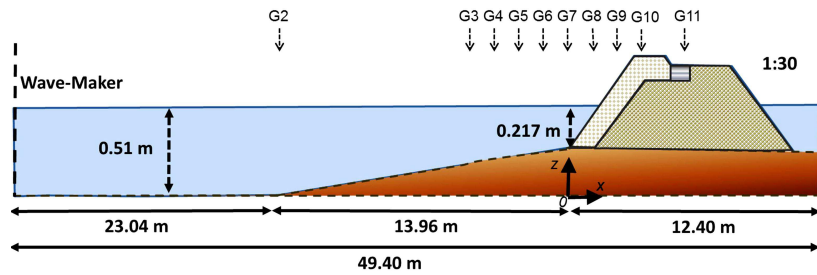


Figure 2. Wave flume profile for the experimental tests (scale 1:30).

The modeled structure was composed by a rock armor layer, with 1.6:3 slope, developed between the crest berm, at +7.0m (CD), and the natural seabed at -3.0m (CD). In the central zone of the breakwater section there was a 3.0m width concrete slab with a crest at +6.5m (CD). The primary armor layer was composed by 90 to 120kN blocks (prototype values). Figure 3 shows the prototype breakwater section and a view of the breakwater at the scale model tests. The porosity of the rock layer was around 40%.

For the experimental tests, waves with different heights (H) and periods (T) were generated. Results for 12s wave period with 2.5m and 3.3m wave heights are presented in this paper.

Table 1 shows the position of the wave gauges along the flume considering the toe of the breakwater as the Oxz referential (Figure 2). Gauge G2 was placed in order to monitor the wave generated by the wave-maker. From G3 to G7 the gauges recorded time series of free surface elevation in front of the structure. Gauges G8 to G10 measured the water level inside and above the rock armor layer. Lastly, gauge G11 was placed on the top center of the concrete impermeable slab to measure the water level. Overtopping volume was obtained using a tank located at the back of the structure and a water level gauge.

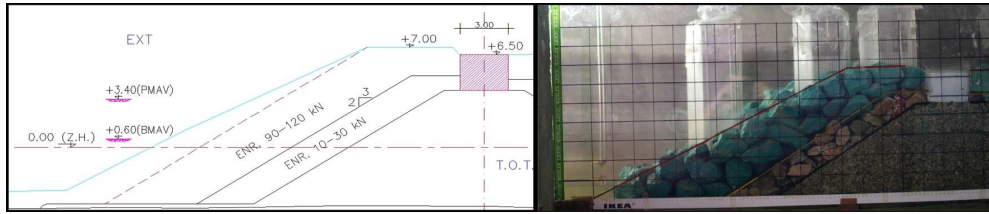


Figure 3. Breakwater section: prototype and at the 1:30 model scale.

Table 1. Gauge positions along the wave flume.

Gauge	G2	G3	G4	G5	G6	G7	G8	G9	G10	G11
x (m)	-13.96	-3.79	-2.53	-2.03	-1.23	-0.055	0.297	0.56	0.745	0.875

4. Results

Coupling section was located at the gauge G5. Spectral analysis of time series of free surface elevation obtained with FLUINCO code at this gauge enables defining the amplitude and phase of the relevant frequencies to transfer to SPHyCE considering the wave transformation along the flume. The breakwater and rock armor layers were modeled with SPHyCE using an impermeable boundary and rectangular blocs. The irregularities of the external rock layer in the experimental set up were estimated to $\pm 0.5\text{cm}$, Figure 3. SPHyCE domain length was less than one wave-length and the resolution, i.e. particle dimension, of 0.18cm was used, corresponding to a total of 202420 particles (Figure 4). The simulation time was 15s and the time step was around $1.5 \times 10^{-5}\text{s}$.

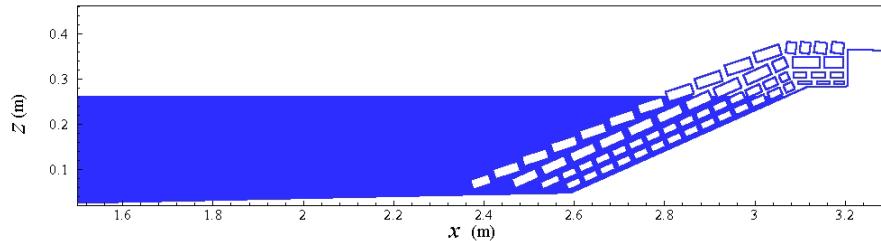


Figure 4. SPH numerical domain and breakwater model.

Figures 5 and 6 show free surface elevation at gauge G6 to G9, for $H=2.5\text{m}$ and 3.3m respectively. Figure 7 shows the water level above the concrete slab and the overtopping volume. Table 2 presents a statistical analysis of the time series of free surface elevation at gauge G6 to G9 for $H=2.5\text{m}$ and 3.3m : *bias* (mean deviation of numerical results compared to experimental data), *rms* (root-mean-square) and *IC* (index of agreement) (Willmott *et al.*, 1985).

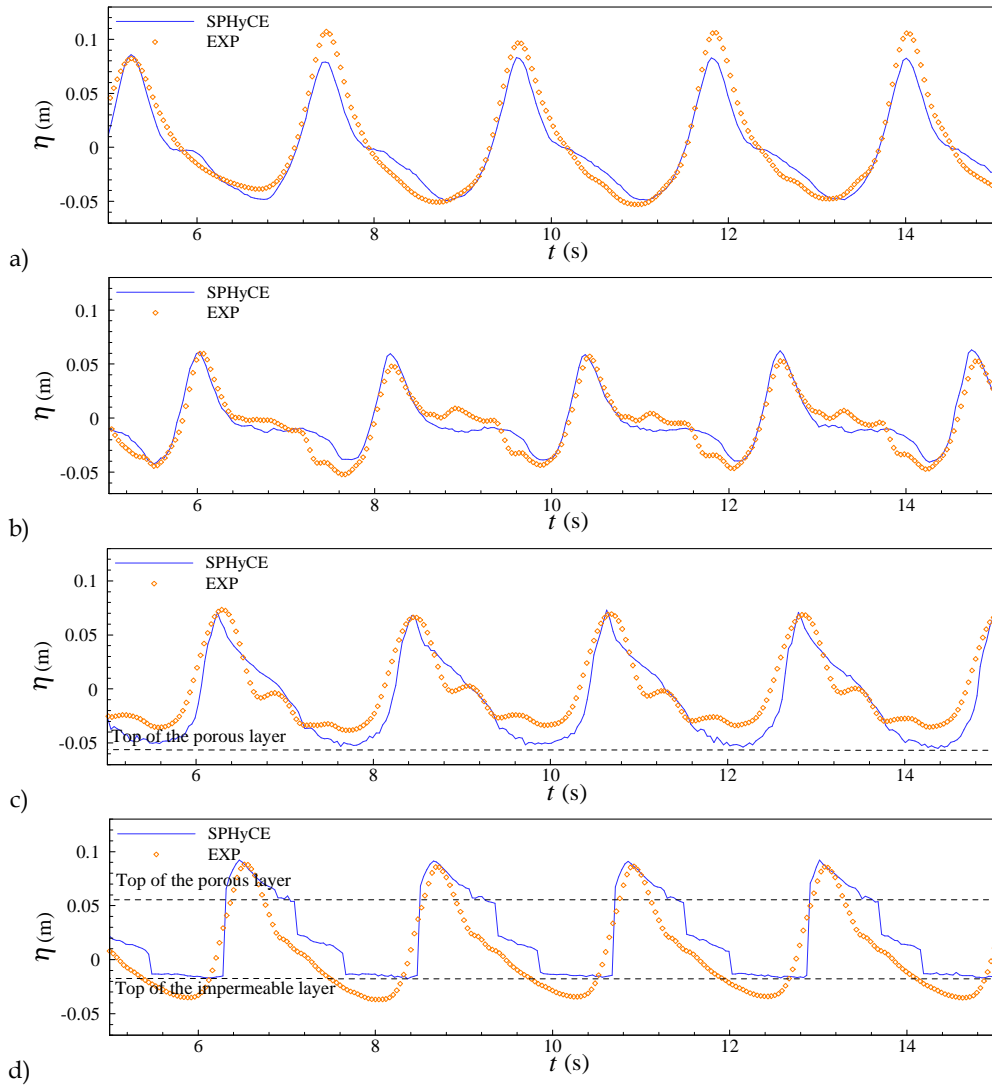


Figure 5. Free surface elevation for $H=2.5$ m (prototype scale): gauge G6 (a), G7 (b), G8 (c), and G9 (d).

In general, the free surface elevation before and inside the breakwater was well estimated, matching the experimental data. For gauge G6, near the wave-maker, free surface elevation was sub-estimated by SPHyCE, *bias* was negative in Table 2, particularly in the wave crests. Probably it is due to small differences in phase between the incident wave characteristics in FLUINCO and the wave generation by the piston wave-maker in SPHyCE. Nevertheless, the free surface at gauge G7 obtained with SPHyCE was in good accordance with the experimental results. Table 2 shows that SPHyCE over-estimates the free surface elevation since *bias* are positive. For $H=2.5$ m and $H=3.3$ m, *IC* is 0.96-0.97, for gauge G6 and G7 respectively, indicating a global good accordance for the time series of free surface elevation.

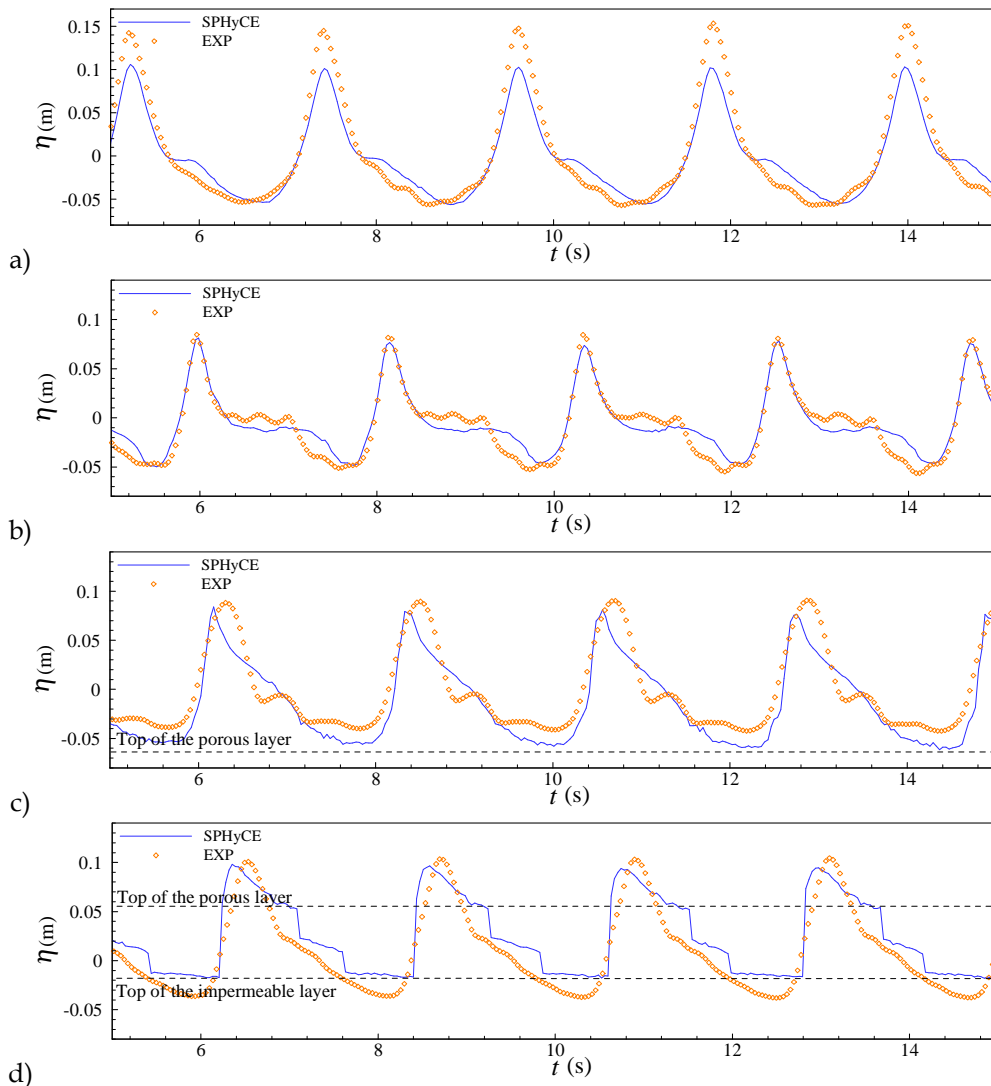


Figure 6. Free surface elevation for $H=3.3$ m (prototype scale): gauge G6 (a), G7 (b), G8 (c), and G9 (d).

Water level at gauges G8 and G9 was well simulated by SPHyCE. The water level above the rock armor layer was in good accordance with the experimental values. Inside the porous layer, numerical results also present a good agreement with the experimental data. Table 2 shows that water level is sub-estimated at gauge G8 but over-estimated at gauge G9. The IC is in the range of 0.90-0.94.

Overtopping volume was well estimated. For $H=2.5$ m there was no overtopping. For $H=3.3$ m the water level at the crest of the breakwater and the duration of the water flow, Figure 7a, was well simulated. Overtopping presents the same trend, Figure 7b, and the difference of overtopping volume per wave between the SPHyCE and the experimental was only of 20%.

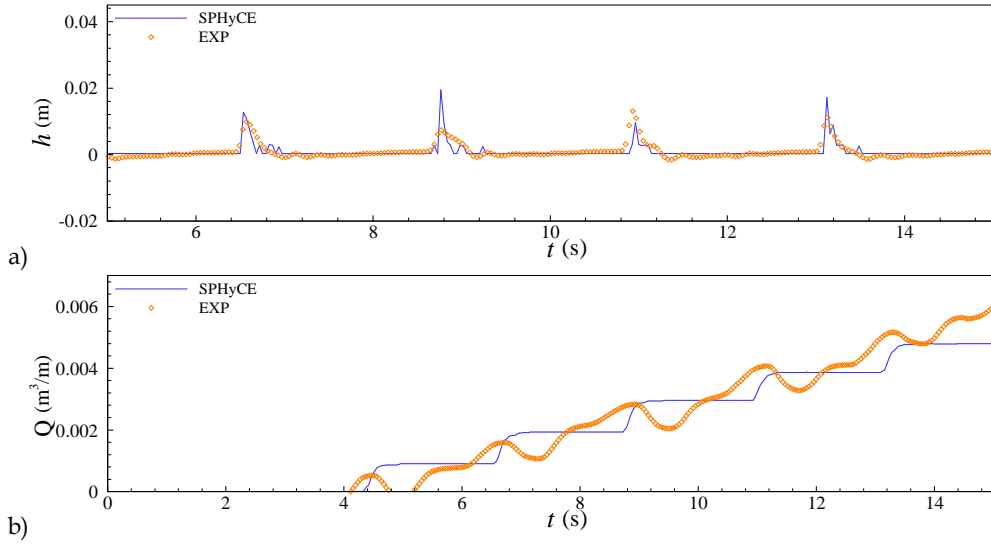


Figure 7. Water level at the concrete slab (a) and overtopping volume (b) for $H=3.3$ m (prototype scale).

Table 2. Statistical parameters of the time series of free surface elevation at gauge G6 to G9 for $H=2.5$ and 3.3 m (prototype scale).

$H=2.5$ m	G6	G7	G8	G9
<i>bias</i>	-0.0038	0.0020	-0.0101	0.0169
<i>rms</i>	0.0130	0.0106	0.0183	0.0230
<i>IC</i>	0.977	0.962	0.931	0.908
$H=3.3$ m	G6	G7	G8	G9
<i>bias</i>	-0.0058	0.0019	-0.0115	0.0155
<i>rms</i>	0.0211	0.0112	0.0193	0.0211
<i>IC</i>	0.961	0.972	0.944	0.934

5. Conclusions

SPHyCE numerical model was applied to simulate wave interaction with a porous breakwater at scale 1:30. The rock armor layers were modeled by rectangular blocks and the irregularities of the external layer were representative of the experimental tests.

Wave propagation in the flume was performed using FLUINCO numerical code. The wave characteristics in the coupling section located at less than one wave-length from the toe of the breakwater were transferred from FLUINCO to SPHyCE numerical code. Free surface elevation before the breakwater and water level inside the rock armor layer were well estimated for the incident wave heights of 2.5 and 3.3 m and wave period of 12 s (prototype values), although some discrepancies appear, probably due to differences in phase between the incident wave characteristics in FLUINCO and the wave generation by the piston wave-maker in SPHyCE. Nevertheless, overtopping was well estimated: there was no overtopping for $H=2.5$ m and the difference of overtopping volume per wave between SPHyCE and the tests for $H=3.3$ m was only 20%, a small value regarding the complexity of this kind of wave-structure interaction.

Acknowledgments

The authors acknowledge the financial support of the Portuguese Foundation for Science and Technology, through project SPACE "A Smoothed Particle Hydrodynamic model development and validation for coastal engineering applications", PTDC/ECM/114109/2009. Eric Didier acknowledges the financial support given by the Portuguese Science and Technology Foundation, SFRH/BPD/37901/2007.

References

- Batchelor G..K., 1974. 'Introduction to Fluid Dynamics', Cambridge University Press, UK.
- Didier E., Neves M.G., 2012. 'A semi-infinite numerical wave flume using Smoothed Particle Hydrodynamics', *IJOPE*, 22(3), 193-199.
- Didier E., Martins R., Neves M.G., 2013. 'Numerical and experimental modeling of regular wave interacting with composite breakwater', *IJOPE*, 23(1), 46-54.
- Gómez-Gesteira M., Rogers B.D., Dalrymple R.A., Crespo A.J.C., Narayanaswamy M., 2008. 'User Guide for the SPHysics Code v1.4', Manchester, UK.
- Gómez-Gesteira M., Rogers B. D., Dalrymple R. A., Crespo A. J. C., 2010. 'State-of-the-art of classical SPH for free-surface flows', *Journal of Hydraulic Research*, 48 Extra Issue, 6-27.
- Gotoh H., Shibahara T., Sakai T., 2001. 'Sub-particle-scale turbulence model for the MPS method - Lagrangian flow model for hydraulic engineering', *Computational Fluid Dynamics Journal*, 9(4), 339-347.
- Johnson G., Stryk R., Beissel S., 1996. 'SPH for high velocity impact calculations', *Computer Methods in Applied Mechanics and Engineering*, 139, 347-373.
- Monaghan J.J., 1994. 'Simulating free surface flows with SPH', *J. Comp. Physics*, 110, 399-406.
- Monaghan J.J., Kos A., 1999. 'Solitary waves on a Cretan beach', *Journal of Waterways, Ports, Coastal and Ocean Engineering*, 125, 145-154.
- Neves D.R.C.B., Didier E., Reis M.T., Neves M.G., 2012. 'Overtopping of a porous structure using a smoothed particle hydrodynamics numerical model', Proc. 4th International Conference on the Application of Physical Modelling to Port and Coastal Protection, Ghent, Belgium.
- Rogers B.D., Dalrymple R.A., 2004. 'SPH modeling of breaking waves', *Proc. 29th Int. Conference on Coastal Engineering*, World Scientific Press, 415-427.
- SPHysics code, version 1.4, 2008. <http://wiki.manchester.ac.uk/sphysics>
- Teixeira P.R.F., Awruch A.M., 2001. 'Three-dimensional simulation of high compressible flows using a multi-time-step integration technique with subcycles', *Applied Mathematical Modelling*, 25, 613-627.
- Teixeira P.R.F., Awruch A.M., 2005. 'Numerical simulation of fluid-structure interaction using the finite element method', *Computer & Fluids*, 34, 249-273.
- Teixeira P.R.F., Fortes C.J.E.M., 2009. 'Aplicação de um modelo numérico não-linear tridimensional na análise de ondas sobre quebra-mares trapezoidais submersos', *Revista Internacional de Métodos Numéricos para Cálculo y Diseño en Ingeniería*, 25(4), 313-336.
- Willmott C.J., Ackleson S.G., Davis R.E., Feddema J.J., Klink K.M., Legates D.R., O'Donnell J., Rowe C.M., 1985. 'Statistics for the evaluation and comparison of models', *Journal of Geophysical Research*, 90(c5), 8995-9005.